One-dimensional conduction properties of highly phosphorus-doped planar nanowires patterned by scanning probe microscopy

Frank J. Rueß,[1,2,*] Bent Weber,[2] Kuan Eng J. Goh,[1,2] Oleh Klochan,[2] Alex R. Hamilton,[2] and Michelle Y. Simmons[1,2]
[1]*Australian Research Council Centre of Excellence for Quantum Computer Technology, School of Physics, University of New South Wales, Sydney, NSW 2052, Australia*
[2]*School of Physics, University of New South Wales, Sydney, NSW 2052, Australia*
(Received 28 December 2006; revised manuscript received 2 April 2007; published 2 August 2007)

We present a detailed study of the cryogenic temperature conduction properties of a low resistivity, highly P-doped nanowire lithographically defined by a scanning tunneling microscope. Temperature-dependent magnetotransport measurements allow us to determine the dominant scattering mechanism as one-dimensional (1D) Nyquist phase breaking. We extract quantum corrections to the Drude conductivity arising from both 1D weak localization and 1D electron-electron interactions for this quasi-1D system. Below 450 mK, the electron phase coherence length is observed to saturate consistent with a Thouless crossover into the strong localization regime.

DOI: 10.1103/PhysRevB.76.085403 PACS number(s): 72.20.−i, 73.20.Fz, 68.37.Ef, 68.65.La

I. INTRODUCTION

Silicon nanowires have recently attracted considerable attention due to their technological potential as sensors, interconnects, and building blocks in silicon-based nanoelectronics. Several strategies to realize narrow wires in silicon have been pursued including top-down fabrication employing a combination of electron beam lithography[1] and reactive ion etching[2] as well as ion-implantation using focused ion beams.[3] However, as devices scale down in size, the wire integrity and uniform definition of its boundary become increasingly challenging with such approaches. A complementary method has been developed based on laser-assisted, catalytic growth[4] of free-standing nanowires. These wires have well-defined boundaries but the conduction is sensitive to the nature of the surface states that surrounds the conducting core.[5]

Recently, we have shown how forming Si:P wires, using a combination of hydrogen resist-based lithography with a scanning tunneling microscope (STM) and Si molecular beam epitaxy (MBE), allows the formation of atomically abrupt nanowires which retain their structural integrity down to at least the ~10 nm level.[6] Using this technique,[7,8] it is possible to define highly planar, P-doped Si nanowires with ultrahigh carrier densities ($\sim 2\times 10^{14}$ cm^{-2}) and, by encapsulation with epitaxial Si, move the conduction electrons away from detrimental surface and interface states. Consequently, such nanowires provide an ideal testbed to study the fundamental limit of conduction in highly disordered Si:P systems.

In earlier work, we showed that lateral confinement of dopants to a 90 nm wire using STM lithography resulted in a demonstration of a crossover from two-dimensional (2D) to one-dimensional (1D) weak localization behavior at low temperature.[7] More recently, resistance saturation has been reported in similar P-doped nanowires down to 50 nm in width.[9] In this work, we specifically address the 1D conduction properties of such wires. For this purpose, we will present a detailed electrical characterization of an STM-defined, 27 nm wide nanowire to determine the quantum corrections to the Drude conductivity.

We use temperature-dependent magnetotransport measurements to extract the dominant dephasing mechanism which is found to be consistent with 1D Nyquist dephasing below 4 K. The total conductance correction is well described by a combination of both 1D weak localization and 1D electron-electron interaction effects. Interestingly, the electron phase coherence length is found to saturate at low temperature for which we propose the onset of a crossover to strong localization consistent with the findings of Gershenson *et al.* in Si δ-doped GaAs wires.[10]

II. SAMPLE FABRICATION AND INITIAL DEVICE CHARACTERIZATION

The 27 nm wide (w) and 320 nm long (L) wire was fabricated on a P-doped (1–10 Ω cm) Si(100) substrate preetched with registration markers[11] to relocate the buried device once the sample is taken outside the ultra high-vacuum (UHV) system. Figure 1(a) shows the wire pattern defined in a hydrogen-resist layer by STM lithography using 6 V and 4 nA as the desorption conditions with a writing speed of 300 nm s^{-1}. The lithographic region appears bright due to the excess tunneling current from the silicon surface states.[12] Note that we can also see the underlying terrace structure of the surface with six atomic steps. We expose this surface to phosphine gas as the dopant precursor which, in conjunction with a thermal anneal, allows the integration of P dopants into the top layer of the silicon substrate defined by STM lithography.[13] We then encapsulate the patterned dopant layer with 25 nm of epitaxial silicon at 250 °C at a rate of 0.5 Å s^{-1} to move the dopants away from the surface states.[14] Buried dopant imaging provides a way to image the dopant region after Si encapsulation and has been shown to demonstrate the structural integrity of such wires below the 10 nm level.[6,8] We also pattern large micron-sized regions at each end of the wire which allow us to align four terminal contacts to the wire using optical lithography as depicted in Fig. 1(b). More details about the device fabrication process can be found in Refs. 7 and 11.

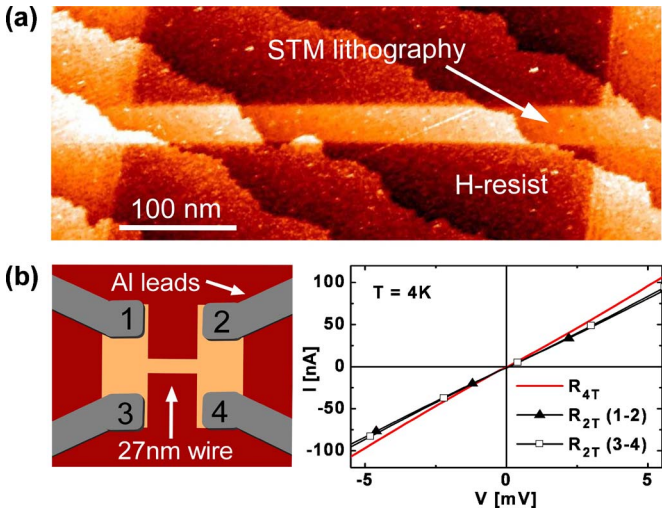

FIG. 1. (Color online) (a) STM image (−2 V, 0.15 nA) of the 27 nm wide wire between contact regions (bright area) after performing STM lithography on a Si(100):H surface. (b) Left-hand side: Schematic view of the contacted wire pattern showing four terminals. Right-hand side: Two- and four-terminal *I-V* characteristics across the wire show low, highly symmetric contact resistances and ohmic conduction with a four-terminal resistance of R_{4T} =50 kΩ at 4 K.

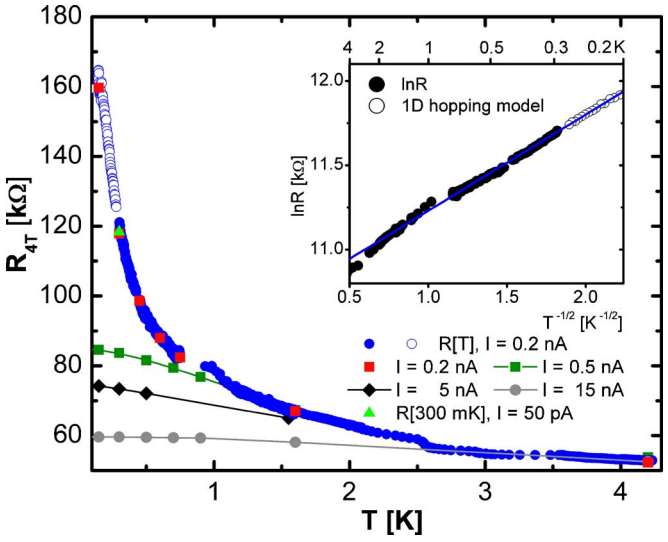

FIG. 2. (Color online) Comparison of the temperature-dependent four-terminal device resistance $R_{4T}[T,I]$ for different currents to illustrate the effect of sample heating. At 4 K, the device resistance is independent of the sample current. For lower temperatures, different sample currents lead to resistance saturation due to Joule heating. For sample currents below 200 pA, the device resistance is independent of the device current down to at least 300 mK. A continuous measurement with a sample current of 0.2 nA [blue (dark) circles] fits well to the individual R_{4T} measurement points at set temperatures. No saturation is observed over the whole measured temperature range down to 150 mK, although current heating cannot completely be ruled out below 300 mK (open circles). Inset: The four-terminal wire resistance follows a 1D variable range hopping model with an extracted value of T_0=330 mK indicating the beginning crossover to strong localization.

Previously, Hall measurements performed on both micron-sized 2D STM-patterned devices[7] as well as δ-doped layers[15] show that we can achieve full activation of the buried P dopants with a carrier density of $\sim 2\times 10^{14}$ cm^{-2}.[16]

Initial device characterization in an Oxford instruments Kelvinox K100 ^{3}H/^{4}He dilution refrigerator is conducted at a bath temperature of 4 K using standard two and four terminal dc techniques. Figure 1(b) shows the two-terminal and four-terminal *I-V* characteristics across the device from which we determine the contact resistances at 4 K. The two-terminal resistances across both sets of contacts (1–2) and (3–4) exhibits a resistance of ~60 kΩ and show a high level of device and contact resistance symmetry. Comparison with the four-terminal resistance of 50 kΩ equates to a low contact resistance of ~5 kΩ per contact.

Ohmic behavior is found for currents up to 100 nA in this device. However at higher currents, we observe the onset of Joule heating in our sample. This corresponds to current densities in excess of 1200 kA/cm^2, where we have assumed a vertical layer thickness of 0.6 nm as determined from separate STM studies.[17] This highlights that care must be taken to eliminate Joule heating at lower temperatures where current heating[18] and electromagnetic noise[19] can result in a saturation of the device resistance and consequently of the electron phase coherence length.

To eradicate the effect of current heating and electromagnetic noise, we performed temperature-dependent calibration measurements using standard ac low-frequency (5 Hz) lock-in techniques using both passive, low-pass filters (Minicircuits BLP 1.9 MHz) and 1 K cold filters with a turnover frequency of 10 kHz. Figure 2 shows the temperature dependence of the four-terminal wire resistance in the range between 150 mK and 4 K for device currents of 0.2, 0.5, 5, and 15 nA, respectively. At 4 K, the sample resistance is found to be independent of the measurement current consistent with the results from the dc *I-V* measurements in Fig. 1(b).

For temperatures below 4 K, we find that sample currents above 0.2 nA cause a saturation of the wire resistance at low temperature, the value of which depends on the level of current heating. Only below 0.2 nA do we find that the sample resistance remains independent of the current down to 300 mK. The wire resistance further increases exponentially and shows no signs of saturation down to 150 mK in contrast to other measurements of narrow STM-patterned P-doped nanowires.[9]

We have fitted the measured resistance to models of hopping conduction,[20,21]

$$R = R_0 \exp\left(\frac{T_0}{T}\right)^{\mu}, \tag{1}$$

where $\mu=\frac{1}{1+d}$ is determined by the effective dimension d of the hopping transport. The inset in Fig. 2 shows a fit to the 1D model, where $\mu=\frac{1}{2}$. The fit gives a value of R_0=43 kΩ which is close to the high-temperature value of R_0=39 kΩ measured at ~50 K. The extracted transition temperature from weak localization to strong localization T_0=330 mK is

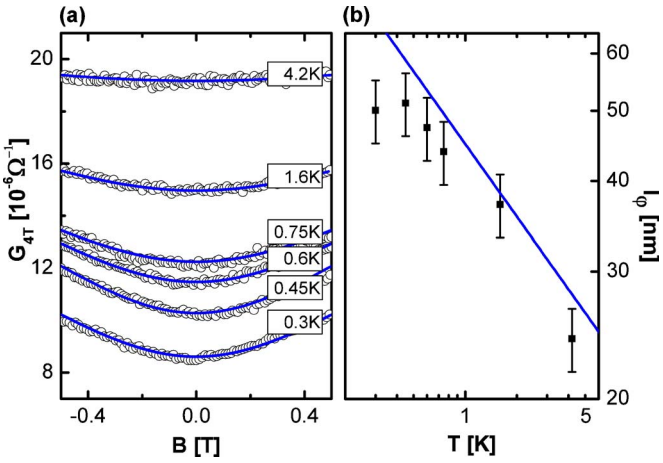

FIG. 3. (Color online) (a) Four-terminal magnetoconductance in the temperature range from 300 mK to 4 K for the 27 nm wire. Solid lines (blue) are fits to 1D weak localization theory (Ref. 24). (b) Temperature-dependent electron phase coherence as obtained from 1D weak localization fitting. The solid line represents the predicted temperature dependence for 1D Nyquist dephasing.

within our measurement range. This suggests that we will observe the onset of a Thouless crossover into the strong localization regime at low temperatures. Note that neither a 2D hopping model $\left(\mu=\frac{1}{3}\right)$ nor a general activation-type hopping model $(\mu=1)$ resulted in good fits.

III. 1D WEAK LOCALIZATION

We have performed temperature-dependent magnetotransport measurements to determine the dominant dephasing mechanism in this highly disordered quasi-1D system. The crucial length scale which governs the strength as well as the dimensionality of weak localization (WL) is the electron phase coherence length l_φ. A transition from 2D to 1D weak localization occurs when the magnitude of l_φ exceeds the wire width w and has previously been observed in a 90 nm wide wire.[7]

While Nyquist dephasing was identified to be the governing dephasing mechanism in 2D P δ-doped layers,[9,22] the effective mechanism in quasi-1D has not been reported for this system to date. Temperature-dependent magnetotransport measurements allow us to determine the effective dimensionality of the wire.

Figure 3(a) shows magnetotransport data between 300 mK and 4 K for a constant device current of 0.2 nA. In previous studies, we used the Hikami formula for 2D WL in a disordered system[23] to extrapolate the phase coherence length of $l_\varphi=24$ nm at 4 K.[6] Below 4 K, however, we found the 2D theory no longer provides a reasonable fit to the data indicating a dimensional crossover from 2D to 1D WL around this temperature for the 27 nm wide wire.

The 1D weak localization correction to the conductance[24] is given by

$$\Delta G_{\mathrm{WL}}(B) = \delta G_{\mathrm{WL}}(B) - \delta G_{\mathrm{WL}}(B=0) = \alpha\frac{2e^2}{hL}\left[l_\varphi - \left(\frac{1}{l_\varphi^2} + \frac{e^2B^2w^2}{3\hbar^2}\right)^{-1/2}\right], \quad (2)$$

where l_φ and α are the only adjustable parameters. We found the dimensionless prefactor α to be unity in our samples consistent with the case of strong intervalley scattering for which a single valley approximation is valid.[25–27]

Figure 3(a) shows good fits to the 1D weak localization model (solid lines) with the corresponding magnetotransport data. At 4 K, we obtain the same l_φ of 24 nm as for the 2D Hikami formula demonstrating that we are indeed in the dimensional crossover regime. Note that the zero-field conductance offset is added to the fits obtained using Eq. (2) to match the measured magnetoconductance. This is done to account for zero-field conductance corrections due to both weak localization and electron-electron interaction, and will be addressed in more detail in the following section. The extracted values of the electron phase coherence length for the 27 nm wide wire are shown from 300 mK to 4 K in Fig. 3(b). We note that l_φ increases up to 450 mK at which point an apparent saturation is observed. Nyquist dephasing due to quasielastic scattering of electrons with a fluctuating electromagnetic field produced by other conduction electrons is believed to be the dominant dephasing mechanism at low temperatures and has been observed by several other groups.[28–33] Altshuler provided an analytical expression for Nyquist dephasing given by

$$l_\varphi = \left(\frac{D\hbar^2 L}{\sqrt{2}R_0 e^2 k_B T}\right)^{1/3}, \quad (3)$$

where D is the diffusion constant and R_0 is an approximation of the Drude resistance. Using $D=5\times10^{-4}$ m^2 s^{-1}, $L=320$ nm, and $R_0=39$ kΩ, we obtain the calculated Nyquist dependence with no adjustable parameters given by $l_\varphi=45\ \mathrm{nm}\times T^{-1/3}$. Figure 3(b) shows good agreement with the experimentally determined phase coherence values down to 450 mK where l_φ starts to saturate. This finding is consistent with a power-law fit to the data between 450 mK and 4 K giving $l_\varphi=40\ \mathrm{nm}\times T^{-0.31}$. 1D Nyquist dephasing can therefore be identified as the dominant phase-breaking mechanism consistent with 2D Nyquist dephasing found in unpatterned P δ-layers.[22] Now that we have established the presence of 1D weak localization, we will investigate the role of electron-electron interactions in this system.

IV. THE INFLUENCE OF 1D ELECTRON-ELECTRON INTERACTIONS ON DEVICE CONDUCTANCE

At low temperatures electron-electron interactions (EEI) effects originating from Coulomb interaction between conduction electrons start to have a considerable impact on the conductance particularly for quasi-1D systems.[34]

From the preceding section, we can determine the effect of weak localization to the total conductance correction $\Delta G_{4T}(T,B=0)=\frac{1}{R(T)}-\frac{1}{R_0}$ in our sample. In the asymptotic limit for $B\to0$, the conductance correction due to WL is

$$\delta G_{\mathrm{WL}}(B=0) = -\frac{2e^2}{hL}l_\varphi. \quad (4)$$

The effective dimensionality of EEI is determined by the magnitude of the thermal length $l_T=\sqrt{\frac{\hbar D}{kT}}$ compared to the wire width.[35] For $l_T>w$ the sample is expected to follow 1D

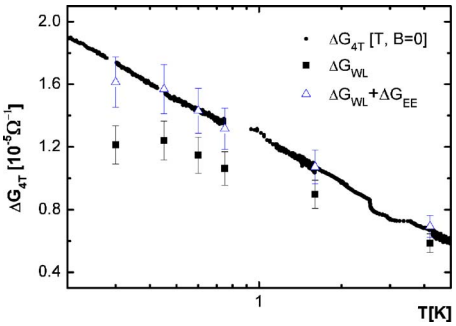

FIG. 4. (Color online) The temperature dependence of the total conduction correction $\Delta G_{4T}(T,B=0)$. The conductance correction is well described by a combined contribution (open triangles) from both 1D weak localization (solid squares) and 1D electron-electron interactions.

EEI theory. In this 27 nm wide wire, we expect a dimensional crossover below ~5 K, where l_T exceeds the wire width.

EEI in a 1D system is expressed by[34,36]

$$\delta G_{\mathrm{EE}} = -\alpha_{ee}\frac{e^2}{\sqrt{2}\pi\hbar L}\frac{4.91}{\pi}l_T, \tag{5}$$

where α_{ee} is an effective screening parameter typically between zero and unity.

By combining Eqs. (4) and (5), we are able to explain the total conductance correction $\Delta G(T)$ by a linear combination of $\delta G_{\mathrm{WL}}+\delta G_{\mathrm{EE}}$ where we have used α_{ee} as a fit parameter.

Figure 4 shows excellent agreement with our data down to a temperature of 450 mK. The extrapolated screening factor α_{ee} of 0.13 is slightly lower than $\alpha_{ee}=0.37$[10] found in wire arrays etched into silicon δ-doped GaAs where conduction also takes place in a highly disordered dopant plane. This highlights that EEI are less pronounced in our system. The dominance of 1D WL is further evidenced by comparing its contribution to the total conductance also shown in Fig. 4.

The apparent saturation of the electron phase coherence length below 450 mK is reflected in the 1D WL contribution and has been observed in other systems.[37–41] We showed that the conductance of the wire is also well described by a 1D variable range hopping (VRH) model which predicts a crossover temperature to strong localization at ~330 mK. The fact that both descriptions can explain the conductance behavior in our wire means that we are in a crossover conduction regime between weak and strong localization.

This crossover occurs when the localization length,[42–44] $\xi=\frac{hL}{2e^2}\frac{1}{R_0}$, becomes comparable to the electron phase coherence length l_φ, i.e., $\xi\sim l_\varphi$.[10] For the 27 nm wide wire, ξ equates to ~100 nm, which is approximately 2 times the value of the coherence length at 450 mK. Khavin *et al.*[10] have also observed a crossover with l_φ 2–3 times smaller than ξ. As such, it is feasible to assume that the 27 nm wire approaches the strongly localized regime at temperatures of $T\sim 330$ mK. A smooth transition into the strong localization regime is expected since both WL and EEI continuously drive a disordered system into its localized state.

V. CONCLUSION

We have investigated the 1D conduction properties of narrow (~25 nm), highly doped, planar nanowires in silicon created with an atomically controlled patterning technique employing STM lithography and low-temperature silicon MBE.

From 1D weak localization measurements, we found that the electron phase breaking rate is due to 1D Nyquist dephasing whereas the total conductance correction could be well described by a combination of both 1D weak localization and 1D electron-electron interaction effects. The conductance of the wire also follows a 1D VRH model with $T_0\sim 330$ mK. Both findings suggest an intermediate conduction regime between weak and strong localization consistent with an apparent saturation of the electron phase coherence length. Future studies on narrower wires are needed to further explore the strong localization regime — a likely candidate to limit conduction in this highly diffusive system as the wire width approaches the atomic scale.

ACKNOWLEDGMENTS

The authors would like to thank Y. Imry and O. Sushkov for fruitful discussions. This work was supported by the Australian Research Council, the Australian Government, the US Advanced Research and Development Activity, National Security Agency, Army Research Office under Contract No. DAAD19-01-1-0653 and the Semiconductor Research Corporation.

*ruess@phys.unsw.edu.au
†URL: http//www.qc-australia.org

[1] S.-J. Park, J. A. Liddle, A. Persaud, F. I. Allen, and T. Schenkel, J. Vac. Sci. Technol. B **22**, 3115 (2004).
[2] L. Pescini, A. Tilke, R. H. Blick, H. Lorenz, J. P. Kotthaus, W. Eberhardt, and D. Kern, Nanotechnology **10**, 418 (1999).
[3] R. A. Smith and H. Ahmed, J. Appl. Phys. **81**, 2699 (1997).
[4] G. Zheng, W. Lu, S. Jin, and C. M. Lieber, Adv. Mater. (Weinheim, Ger.) **16**, 1890 (2004).
[5] J. B. Hannon, S. Kodambaka, F. M. Ross, and R. M. Tromp, Nature (London) **440**, 69 (2006).
[6] F. J. Rueß, K. E. J. Goh, M. J. Butcher, T. C. G. Reusch, L. Oberbeck, B. Weber, A. R. Hamilton, and M. Y. Simmons, Nanotechnology **18**, 044023 (2007).
[7] F. J. Rueß, L. Oberbeck, M. Y. Simmons, K. E. J. Goh, A. R. Hamilton, T. Hallam, S. R. Schofield, N. J. Curson, and R. G. Clark, Nano Lett. **4**, 1969 (2004).
[8] F. J. Rueß, W. Pok, T. C. G. Reusch, M. J. Butcher, K. E. J. Goh,

L. Oberbeck, G. Scappucci, A. R. Hamilton, and M. Y. Simmons, Small **3**, 563 (2007).
[9] S. J. Robinson, J. S. Kline, H. J. Wheelwright, J. R. Tucker, C. L. Yang, R. R. Du, B. E. Volland, I. W. Rangelow, and T.-C. Shen, Phys. Rev. B **74**, 153311 (2006).
[10] Y. B. Khavin, M. E. Gershenson, and A. L. Bogdanov, Phys. Rev. B **58**, 8009 (1982).
[11] F. J. Rueß, L. Oberbeck, K. E. J. Goh, M. J. Butcher, E. Gauja, A. R. Hamilton, and M. Y. Simmons, Nanotechnology **16**, 2446 (2005).
[12] R. J. Hamers, P. Avouris, and F. Bozso, Phys. Rev. Lett. **59**, 2071 (1987).
[13] S. R. Schofield, N. J. Curson, M. Y. Simmons, F. J. Rueß, T. Hallam, L. Oberbeck, and R. G. Clark, Phys. Rev. Lett. **91**, 136104 (2003).
[14] L. Oberbeck, N. J. Curson, M. Y. Simmons, R. Brenner, A. R. Hamilton, and R. G. Clark, Appl. Phys. Lett. **81**, 3197 (2002).
[15] K. E. J. Goh, L. Oberbeck, M. Y. Simmons, A. R. Hamilton, and R. G. Clark, Appl. Phys. Lett. **85**, 4953 (2004).
[16] Note that we can confirm that conduction in the wire originates from the buried dopants by simultaneously measuring a control device which consists of a four terminal contact structure on the same chip without any STM patterning. The control device gave a resistance in excess of 100 MΩ indicating that the hydrogen resist prevents dopant adsorption in the unpatterned regions.
[17] L. Oberbeck, N. J. Curson, T. Hallam, M. Y. Simmons, and R. G. Clark, Appl. Phys. Lett. **85**, 1359 (2004).
[18] O. Prus, M. Reznikov, U. Sivan, and V. Pudalov, Phys. Rev. Lett. **88**, 016801 (2001).
[19] B. L. Altshuler, M. E. Gershenson, and I. L. Aleiner, Physica E (Amsterdam) **3**, 58 (1998).
[20] A. B. Fowler, A. Hartstein, and R. A. Webb, Phys. Rev. Lett. **48**, 196 (1982).
[21] B. I. Shklovskii and A. L. Efros, *Electronic Properties of Doped Semiconductors*, Springer Series in Solid-State Sciences (Springer-Verlag, Berlin, 1984).
[22] K. E. J. Goh, Ph.D. thesis, University of New South Wales, Sydney, Australia, 2007.
[23] S. Hikami, A. I. Larkin, and Y. Nagaoka, Prog. Theor. Phys. **63**, 707 (1980).
[24] B. L. Altshuler, A. G. Aronov, and D. E. Khmelnitsky, J. Phys. C **15**, 7367 (1982).
[25] H. Fukuyama, Surf. Sci. **113**, 489 (1982).
[26] N. L. Mattey, T. E. Whal, R. A. Kubiak, and M. J. Kearney, Semicond. Sci. Technol. **7**, 604 (1992).
[27] K. E. J. Goh, L. Oberbeck, M. Y. Simmons, A. R. Hamilton, and M. J. Butcher, Phys. Rev. B **73**, 035401 (2006).
[28] M. E. Gershenson, Y. B. Khavin, A. G. Mikhalchuk, H. M. Bozler, and A. L. Bogdanov, Phys. Rev. Lett. **79**, 725 (1997).
[29] F. Pierre, A. B. Gougam, A. Anthore, H. Pothier, D. Esteve, and N. O. Birge, Phys. Rev. B **68**, 085413 (2003).
[30] S. Wind, M. J. Rooks, V. Chandrasekhar, and D. E. Prober, Phys. Rev. Lett. **57**, 633 (1986).
[31] D. Natelson, R. L. Willett, K. W. West, and L. N. Pfeiffer, Phys. Rev. Lett. **86**, 1821 (2001).
[32] J. J. Lin and N. Giordano, Phys. Rev. B **35**, 545 (1987).
[33] K. Liu, P. Avouris, R. Martel, and W. K. Hsu, Phys. Rev. B **63**, 161404(R) (2001).
[34] B. L. Altshuler and A. G. Aronov, *Electron-Electron Interations in Disordered Systems* (North-Holland, Amsterdam, 1985).
[35] C. W. J. Beenakker and H. van Houten, Solid State Phys. **44**, 1 (1991).
[36] P. A. Lee and T. V. Ramakrishnan, Rev. Mod. Phys. **57**, 287 (1985).
[37] Y. B. Khavin, M. E. Gershenson, and A. L. Bogdanov, Phys. Rev. Lett. **81**, 1066 (1998).
[38] J. J. Lin and N. Giordano, Phys. Rev. B **35**, 1071 (1986).
[39] D. M. Pooke, N. Paquin, M. Pepper, and A. Gundlach, J. Phys.: Condens. Matter **1**, 3289 (1989).
[40] P. Mohanty, E. M. Q. Jariwala, and R. A. Webb, Phys. Rev. Lett. **78**, 3366 (1996).
[41] J. J. Lin and J. P. Bird, J. Phys.: Condens. Matter **14**, R501 (2002).
[42] D. J. Thouless, Phys. Rev. Lett. **39**, 1167 (1977).
[43] P. W. Anderson, Phys. Rev. **109**, 1492 (1958).
[44] E. Abrahams, P. W. Anderson, D. C. Licciardello, and T. V. Ramakrishnan, Phys. Rev. Lett. **42**, 673 (1979).